Available on CMS information server

CMS CR-2008/054

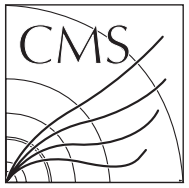

The Compact Muon Solenoid Experiment

Conference Report

Mailing address: CMS CERN, CH-1211 GENEVA 23, Switzerland

06 August 2008

LHC Capabilities for Quarkonia

Sergey Petrushanko

Abstract

The measurement of the charmonium and bottomonium resonances in nucleus-nucleus collisions provides crucial information on high-density QCD matter. First, the suppression of quarkonia production is generally agreed to be one of the most direct probes of quark-gluon plasma formation. The observation of anomalous J/ψ suppression at the CERN-SPS and at RHIC is well established but the clarification of some important remaining questions requires equivalent studies of the Υ family, only possible at the LHC energies. Second, the production of heavy-quarks proceeds mainly via gluon-gluon fusion processes and, as such, is sensitive to saturation of the gluon density at low-x in the nucleus. Measured departures from the expected vacuum quarkonia cross-sections in Pb+Pb collisions at the LHC will thus provide valuable information not only on the thermodynamical state of the produced partonic medium, but also on the initial-state modifications of the nuclear parton distribution functions. The capabilities of the LHC detectors (ALICE, ATLAS and CMS) to study quarkonia production in Pb+Pb collisions at 5.5 TeV per nucleon pair are discussed.

Presented at *Hard Probes 2008, June 8-14, 2008, Illa da Toxa, Spain*

1 Introduction

The suppression of heavy quark-antiquark bound states with increasing energy density due to Debye screening of the colour potential in the plasma is generally agreed to be one of the most direct probes of Quark-Gluon-Plasma formation [1].

The CERN SPS results [2, 3] showed a strong anomalous suppression of J/ψ production in Pb+Pb and In+In collisions at c.m.s. energy per nucleon pair $\sqrt{s_{NN}} = 17.3$ GeV. The further study of J/ψ production at $\sqrt{s_{NN}} = 200$ GeV in Au+Au [4] and Cu+Cu [5] collisions at RHIC revealed a global J/ψ suppression of a factor 3. between most central and peripheral collisions which can be explained only partially by calculations including shadowing and absorption [6]. As for Υ production, the cross-section is large enough to be observed at RHIC, with limited statistics, but its suppression is not expected until the high initial temperatures foreseen at LHC are reached.

Recent theoretical analyses [7] show that the direct J/ψ could survive upto temperatures as high as 1.5 T_c (the critical temperature for the phase transition, about 200 MeV) which could be out of range at RHIC. At RHIC and LHC energies a possible regeneration of the J/ψ, due to the large production of $c\bar{c}$ pairs, may compensate an anomalous suppression [8].

We summarise here the capabilities of ALICE, ATLAS and CMS detectors at the LHC to study quarkonia production in Pb+Pb collisions at $\sqrt{s_{NN}} = 5.5$ TeV.

2 ALICE

2.1 ALICE detector

ALICE will be the only dedicated heavy-ion experiment at the LHC [9]. It was optimized to measure a large variety of heavy-ion observables at the LHC energy. Besides others, the measurement of quarkonia is a key element of the ALICE physics program. The ALICE central detectors are embedded in a large magnet (L3) providing a weak solenoidal magnetic field (< 0.5 T).

Quarkonia will be detected in ALICE via the decays into both dielectrons and dimuons, in the central barrel and forward muon spectrometer respectively. The combined measurement at central and forward rapidities will allow to probe a continuous range of Bjorken-x with values as low as 10^{-5}, shedding more light on the scale dependence of parton densities in the small-x regime.

Dielectronic decays of quarkonia will be measured in the central barrel (pseudorapidity region $|\eta| < 0.9$) involving the following three detectors:

Inner Tracking System (ITS)
The Inner Tracking System consists of three different types of silicon detectors, a silicon pixel detector (SPD), a silicon strip detector (SSD) and a silicon drift detector (SDD) arranged in six layers around the beam axis. The resolution of the combined ITS is ~ 70 μm in rϕ and $\sim 170\mu$m in z at transverse momentum $p_T = 1$ GeV/c, and ~ 20 μm (60 μm) at $p_T = 10$ GeV/c.

Time Projection Chamber (TPC)
With a diameter of ~ 5 m, a length of ~ 5 m and a volume of more than 95 m^3 the ALICE Time Projection Chamber is the largest TPC ever built. It is the main tracking device of the experiment with a momentum resolution of less than 2.5% for electron tracks with $p_T = 4$ GeV/c. Besides that, it will also serve as a particle identification detector using the specific energy loss of particles in the TPC gas (90% Ne, 10% CO_2).

Transition Radiation Detector (TRD)
The Transition Radiation Detector was added to the experiment to improve the tracking capabilities and to discriminate electrons from the huge background of pions and other hadrons. The TRD will also serve as a fast trigger device for high p_T electrons. It cylindrically surrounds the TPC with an inner diameter of ~ 6 m and an outer diameter of ~ 6.8 m and is segmented into 18 super modules. Each of these super modules is segmented in 5 stacks in z-direction with 6 layers of readout chambers in radial direction per stack. This gives a total of 540 read out chambers covering an area of 736 m^2 with 1.16 million readout channels.

Quarkonia decaying into dimuons will be measured in the muon arm, covering forward pseudorapidity ($-4 < \eta <$

-2.5) [10]. The ALICE muon spectrometer consists of a passive front absorber of total thickness corresponding to 10 interaction lengths to absorb hadrons and photons from the collision, a high-granularity tracking system of 10 planes of cathode pad chambers, a large dipole magnet creating a field of 0.7 T, and a trigger system made of four planes of resistive plate chambers performing the selection of high transverse momentum muons. Muons penetrating the whole spectrometer length are measured with a momentum resolution of about $1-2$ %.

2.2 ALICE: Dielectron channel

All presented studies were done within the ALICE offline software framework *aliroot* [11] with the fast simulation [12]. Fig. 1 shows the dimuon invariant mass distribution for Pb+Pb collisions in dielectron channel. 2×10^8 central Pb+Pb events were simulated representing the expected statistics for one ALICE running year [13]. A single electron p_T cut of 1 GeV/c was applied. To account for electrons coming from semi-leptonic charm and beauty decays 100 $c\bar{c}$ and 4 $b\bar{b}$ per event were embedded. Pionic background was simulated using a parameterized HIJING generator [14] tuned to the charged particle multiplicity per unit of pseudorapidity $dN_{ch}/d\eta = 3000$. There are significant signals for the J/ψ, Υ and Υ'. ψ' and Υ'' have only small contributions above background. The background was estimated using like-sign pairs. After subtraction of the background and fitting the peaks with a Gaussian one obtains a width of 30 MeV/c^2 for the J/ψ and 90 MeV/c^2 for the Υ sufficient to resolve the individual Υ states. All dielectron channel results are summarized in Table 1.

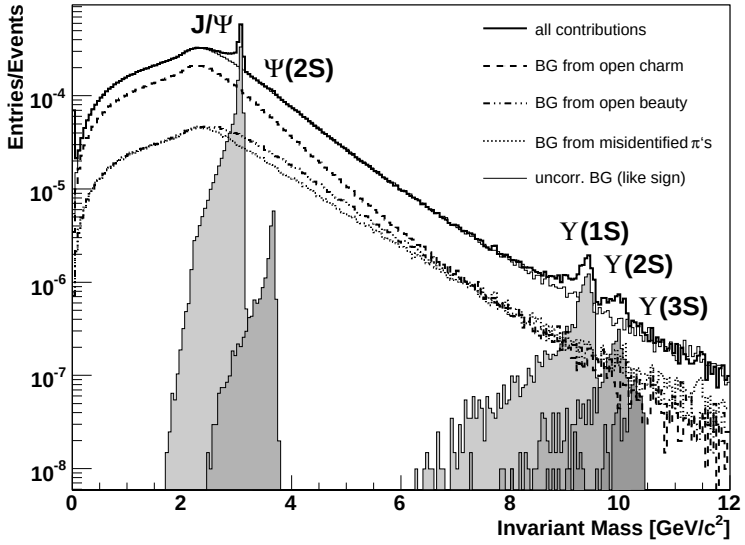

Figure 1: ALICE detector. Invariant mass distribution as expected for 2×10^8 central Pb+Pb collisions. The solid black line shows the unlike-sign distribution. The background was estimated using like-sign pairs (thin black line). The grey areas indicate the pure quarkonia distributions. The dashed lines show the various contributions from other sources to the distributions.

The expected performance of the quarkonia measurement in the dielectron channel has been simulated under realistic assumptions. Within one year of running ALICE will accumulate enough statistics to measure Υ and Υ' in Pb+Pb collisions with good signal-to-background ratio and significance. The invariant mass resolution is sufficient to resolve the individual Υ states. The invariant mass spectrum in the J/ψ and Υ mass region are shown on Fig. 2.

2.3 ALICE: Dimuon channel

Dimuons will be detected in ALICE by the forward muon spectrometer. The invariant mass resolution for the J/ψ peak will be 70 MeV/c^2, and for the Υ peak will be 100 MeV/c^2. After one ALICE year of data taking the numbers of collected J/ψ, Υ, Υ', Υ'' will be 670000, 7000, 2000 and 1000, respectively. The opposite-sign dimuon mass yeilds for the J/ψ and Υ regions are shown on the Fig. 3, corresponding to the 4.4% most central Pb+Pb collisions. Signals are fitted with Landau convoluted Gaussian function and no suppression or enhancement been assumed.

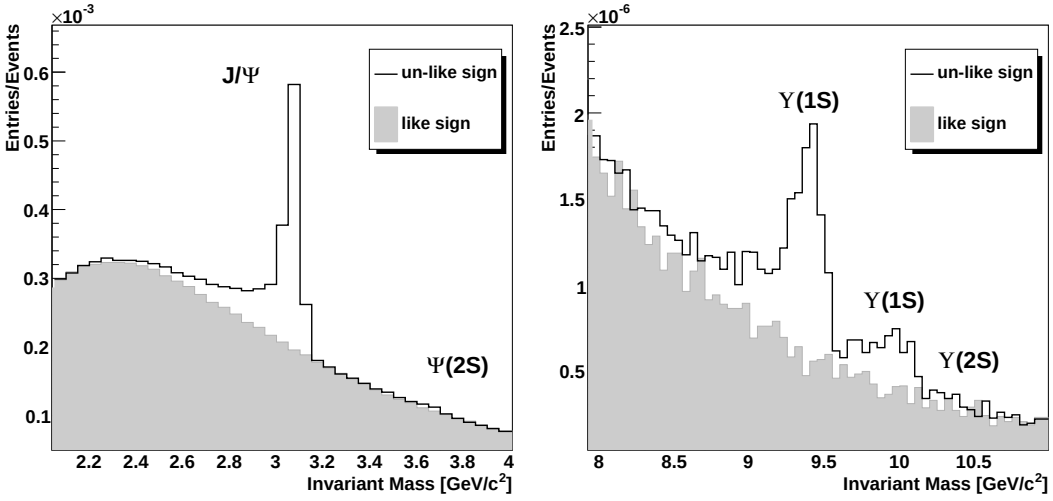

Figure 2: ALICE detector. The invariant mass spectrum in the J/ψ (left) and Υ (right) mass regions for one running year.

Table 1: ALICE detector. Summary of the main results for dielectron channel of quarkonia in central Pb+Pb collisions (statistics is for one running year).

	J/ψ	Υ	Υ'
signals	120000	900	350
S/B	1.2	1.1	0.35
$S/\sqrt{S+B}$	245	21	8

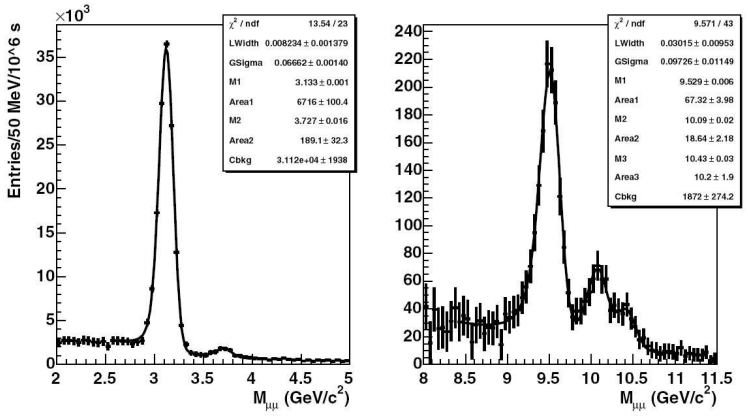

Figure 3: ALICE detector. Fits of the opposite-sign dimuon mass yields for the J/ψ (left) and Υ (right) mass regions, corresponding to the 4.4% most central Pb+Pb collisions, without suppressions or enhancements.

2.4 ALICE: Conclusions

It will be possible to resolve the complete quarkonium spectrum (J/ψ, ψ', Υ, Υ', Υ'') with the expected invariant mass resolutions. For charmonium states the expected signal-to-background ratios are relatively small but the expected signal significance is high thanks to the large statistics available. For the Υ, the expected signal is roughly two order of magnitude lower that the J/ψ. At the same time, in this high-mass region the background is lower by around three orders of magnitude, resulting in a signal significance of ~ 20 for a one year data taking period. For Υ, Υ' and Υ'', even if signal statistics are tight, good performance is still expected. The expected available statistics after one year of data taking, should enable to study the centrality dependence of the hidden-to-open heavy flavour ratios (Υ to opposite sign muon pairs from beauty decays) and the p_T dependence of quarkonium production, needed to constrain QGP models and suppression scenarios.

3 ATLAS

3.1 ATLAS detector

The ATLAS detector [15, 16] is a large, multi-purpose detector designed for detecting and reconstructing high-p_T observables in pp collisions. It is composed of an inner tracking system, electromagnetic and hadron calorimeters, and a muon spectrometer. Even though ATLAS was designed for pp multiplicities, expected occupancies for central Pb+Pb events are low enough for most subsystems to be used as a heavy-ion detector [17].

The inner tracking system covers full azimuth and approximately $|\eta| < 2.5$ and is within a 2 T solenoidal field. It consists of three pixel layers (r $= 50.5$ mm, 88.5 mm and 122.5 mm), followed outward by four layers of double-sided silicon strip detectors, and finally the transition radiation tracker a straw tracker with 35 points for $|\eta| < 2.5$ and $p_T > 0.5$ GeV/c. The occupancies of the pixel layers and the silicon strips are less than 2% and 20% for central Pb+Pb events. However, the occupancy for the transition radiation tracker is large. As such, heavy-ion tracking is being optimized with the 11 space points from the pixels and the strips.

The calorimeter coverage in ATLAS is full azimuth and $|\eta| < 5$ with several radial (longitudinal) segments. The barrel region ($|\eta| < 1.5$) calorimeter consists of a thin presampler to measure lost energy in material before the calorimeter, three longitudinal segments of liquid argon (LAr) electromagnetic calorimeters, and three longitudinal segments of tile hadronic calorimeters. The endcap calorimeter region ($1.5 < |\eta| < 3.2$) is composed of the same LAr electromagnetic calorimetry as the barrel, while the hadronic calorimeter consists of two longitudinal segments of copper plates. Finally the forward ($3.2 < |\eta| < 4.9$) hadronic calorimeter has three segments.

Beyond the hadronic calorimeters and within a toroidal field is the muon spectrometer, the largest ever constructed, with acceptance of muons out to $|\eta| < 2.7$. It consists of three chambers containing drift tubes (in the midrapidity, barrel region) or cathode strip chambers (in the forward rapidities) to measure the position of the tracks passing through the chambers. The occupancy is very low since the hadronic calorimeters absorb nearly all the hadron background.

3.2 ATLAS: Upsilon measurements

The possibility to measure the Υ and J/ψ quarkonium families via dimuon decays in heavy-ion collisions with the ATLAS experiment has been studied in [18]. The full reconstruction chain of the ATLAS analysis package "Athena" version 12.0.6 was used to study single Υ's embedded in central (impact parameter $b = 2$ fm) Pb+Pb HIJING events [14].

The Υ mass resolution in Pb+Pb events as a function of η is shown in Fig. 4 (left). On the same plot single Υ mass resolution (without any background) was shown. No deterioration of mass resolution in central Pb+Pb events compared to single Υ's is observed. The best mass resolution of ≈ 120 MeV is achieved in the barrel region ($|\eta| < 1$). There is a weak p_T dependence of mass resolution, which is expected from large Υ mass. Mass resolution can be further improved by restricting the η of decay muons and by tightening reconstruction cuts. This, however, results in Υ yield reduction.

To study reconstruction efficiency in a high multiplicity environment, single Υ's merged with central ($b = 2$ fm) Pb+Pb HIJING events were compared with the same single Υ's merged with PYTHIA pp events.

Reconstruction efficiency times acceptance ($A \times \varepsilon$) in central ($b = 2$ fm) Pb+Pb events is shown in Fig. 4 (right). Integrated over p_T and η, the $A \times \varepsilon$ for these events is $10.5\% \pm 0.1\%$, while in pp events it is $12.3\% \pm 0.1\%$. Thus, the efficiency in central Pb+Pb events relative to pp events is $\approx 85\%$.

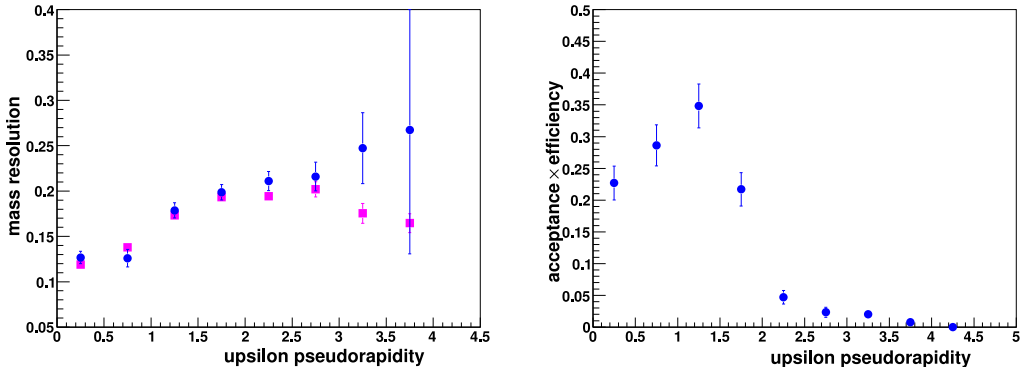

Figure 4: ATLAS detector. Left: Υ mass resolution in central Pb+Pb events as a function of η (circles). For comparison, mass resolution for single Υ (without Pb+Pb events) is shown by the squares. Right: Υ acceptance times efficiency in central Pb+Pb events as a function of η.

The expected dimuon invariant mass distribution is shown in Fig. 5. It corresponds to 24 days of Pb+Pb beamtime assuming 3 kHz collision rate. This plot includes acceptance and efficiency corrections, and is for the barrel region only ($|\eta| < 1$). About 15000 Υ's are expected to be reconstructed. Υ and Υ' states can be clearly separated. Separation for Υ'' states is less clear, but from a physics point of view it is less important since these two states are expected to dissociate at similar temperatures. Signal-to-background ratio for Υ is close to 1.

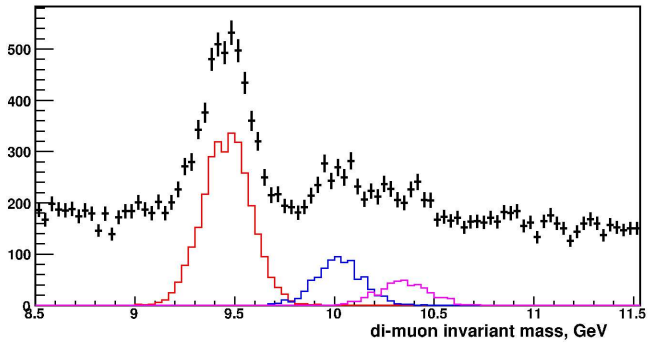

Figure 5: ATLAS detector. Dimuon invariant mass distribution expected for 24 days of Pb+Pb beamtime, at 3 kHz collision rate. Acceptance and efficiency corrected. For barrel region only ($|\eta| < 1$). Solid histograms represent expected yields for the Υ states.

3.3 ATLAS: Charmonium measurements

Charmonium measurement will give additional valuable information about quarkonia suppression. The present charmonium simulation was performed using ATLSIM 7.5.0 package, and GEANT3 (see [19]).

The main problem one faces when measuring J/ψ with the ATLAS detector is the low J/ψ acceptance at low p_T, since muons can be reconstructed only if they have an energy greater than about 2.5 GeV. In order to improve the J/ψ acceptance we considered two alternative methods of muon reconstruction. The first (standard) method requires a muon to fully traverse the ATLAS muon spectrometer, and only such muon tracks are then associated with the tracks from the inner detector. The second method, called "tagging method", requires a muon to pass only through the first two muon stations. Muon tracks are then associated with the tracks in the inner detector. This second method results in worse momentum resolution for muons and more background, but allows the reconstruction of muons with lower p_T, and increases acceptance for J/ψ several times.

Fig. 6 shows the expected reconstructed dimuon invariant mass distribution after approximately one month of beamtime. The expected signal-to-background ratio is close to 0.2.

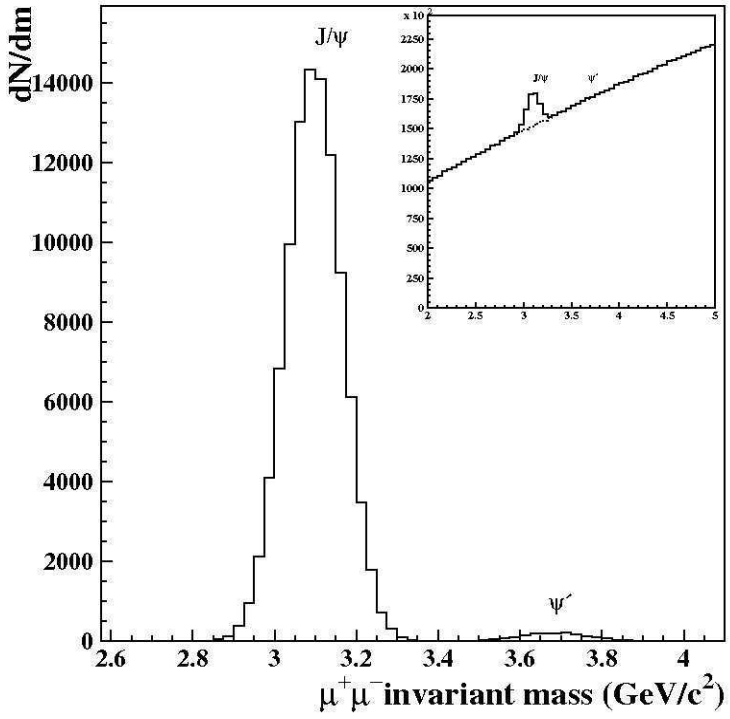

Figure 6: ATLAS detector. J/ψ mass resolution obtained using "tagging method" for one month of Pb+Pb beamtime. On insert: expected dimuon invariant mass distribution.

3.4 ATLAS: Conclusions

In the ATLAS detector the Υ reconstruction efficiency in heavy-ion collisions is only weakly affected by the high multiplicity environment, even in most central Pb+Pb events. Υ mass resolution is good enough to separate Υ and Υ' states, at least in the barrel region ($|\eta| < 1$). Separation for Υ'' states is less clear, but also possible.

Backgrounds for both charmonium and bottomonium are estimated to be at reasonable levels. Signal-to-background ratio for Υ is expected to be close to 1, and ≈ 0.2 for J/ψ. ATLAS expects to see Υ and J/ψ peak in one month of beamtime and reconstruct ≈ 15000 Υ and ≈ 100000 J/ψ (using "tagging method").

4 CMS

4.1 CMS detector

The CMS detector is designed to identify and measure muons, electrons, photons and jets over a large energy and rapidity range. CMS is particularly well suited to study the Υ and J/ψ families, the continuum up to the Z^0 mass and higher masses through the dimuon decay channel.

A detailed description of the detector elements can be found in the corresponding Technical Design Reports [20, 21, 22, 23].

The central element of CMS is the magnet, a 13 m long, 6 m diameter, high-field solenoid (a uniform 4 T field) with an internal radius of ≈ 3 m.

The tracker covers the pseudorapidity region $|\eta| < 2.5$. Starting from the beam axis the tracker is composed of two different types of detectors: pixels and silicon strips. The pixel detector consists of 3 barrel layers located at 4, 7, 11 cm from the beam axis with granularity 150×150 μm^2 and 2 forward layers with granularity 150×300 μm^2 located at the distances of 34 and 43 cm in z-direction from the center of detector. Silicon strip detectors are divided into inner and outer sections and fill the tracker area from 20 cm to 110 cm (10 layers) in the transverse direction and up to 260 cm (12 layers) in longitudinal direction.

The hadronic (HCAL) and electromagnetic (ECAL) calorimeters are located inside the coil (except the forward calorimeter) and cover (including the forward calorimeter) from -5.2 to 5.2 in pseudorapidity. The HF calorimeter

covers the region $3 < |\eta| < 5.2$. The impact parameter (centrality) of the collision can be determined from measurements of transverse energy production over the range $|\eta| < 5.2$.

The number of nuclear interactions length before the muon stations (λ) is $11-16$ over $|\eta| < 3$ [24]. Muons loose 3 GeV in the calorimeter due to ionization losses. The probability for hadrons to not interact in the calorimeter at all is only 0.005%. The first absorber, the electromagnetic calorimeter, is 1.3 m from the interaction point, eliminating a large fraction of the hadronic background.

The CMS muon stations cover the pseudorapidity region $|\eta| < 2.4$ and consist of drift tube chambers (DT) in the barrel region (MB), $|\eta| < 1.2$, cathode strip chambers (CSCs) in the endcap regions (ME), $0.9 < |\eta| < 2.4$, and resistive plate chambers (RPCs) in both barrel and endcaps, for $|\eta| < 2.1$. The RPC detector is dedicated to triggering, while the DT and CSC detectors, used for precise momentum measurements, also have the capability to self-trigger up to $|\eta| < 2.1$.

4.2 CMS: Simulation and analysis of J/ψ and Υ

Having large muon detector acceptance and high precision tracker, the CMS detector is particularly well suited to study the quarkonia state production in the dimuon channel [25, 26]. Event generator HIJING [14] with the official tools of the CMS Collaboration based on GEANT4 for the tracking of secondaries and simulated detector response were used.

The J/ψ and Υ acceptances on CMS are shown as a function of p_T in Fig. 7 for two η ranges: full detector ($|\eta| < 2.4$) and central barrel ($|\eta| < 0.8$). Because of their relatively small mass, low momentum J/ψ's ($p < 4$ GeV/c) are mostly not accepted: their decay muons do not have enough energy to traverse the calorimeters and coil, and are absorbed before reaching the muon chambers. The J/ψ acceptance increases with p_T, flattening out at $\sim 15\%$ for $p_T > 12$ GeV/c. The Υ acceptance starts at $\sim 40\%$ at $p_T = 0$ GeV/c and remains constant at $\sim 15\%$ (full detector) or 5% (barrel only) for $p_T > 4$ GeV/c. The p_T-integrated acceptance is about 1.2% for the J/ψ and 26% for the Υ, assuming the input theoretical distributions.

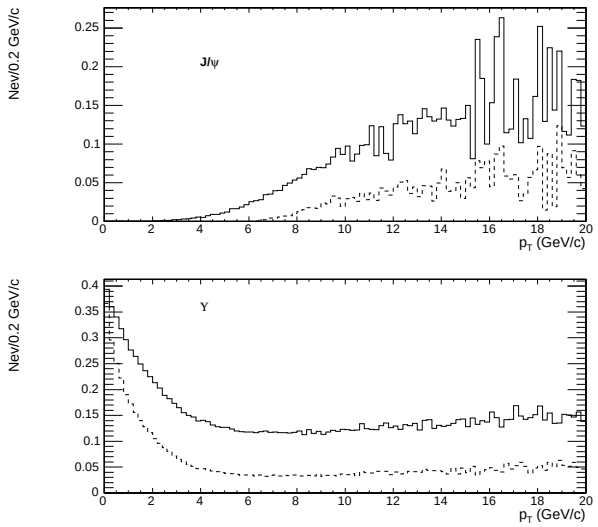

Figure 7: CMS detector: J/ψ (top) and Υ (bottom) acceptances (convoluted with trigger efficiencies) as a function of p_T, in the full detector (barrel and endcap, $|\eta| < 2.4$, solid line) and only in the barrel ($|\eta| < 0.8$, dashed line).

In the central barrel of the CMS detector, the dimuon reconstruction efficiency remains above 80% for all multiplicities whereas the purity decreases slightly with increasing multiplicities $dN_{ch}/d\eta$ but also stays above 80% even at as high as $dN_{ch}/d\eta = 6500$. If (at least) one of the muons is detected in the endcaps, the efficiency and purity drop due to stronger reconstruction cuts. Nevertheless, for the $dN_{ch}/d\eta \approx 2000$ multiplicity realistically expected in central Pb+Pb at LHC, the efficiency (purity) remains above 65% (90%) even including the endcaps.

At the Υ mass, the dimuon mass resolution for muon pairs in the central barrel, $|\eta| < 0.8$, is 54 MeV/c^2. In the full pseudorapidity range, the dimuon mass resolution is about 1% of the quarkonium mass: 35 MeV/c^2 at the J/ψ mass and 86 MeV/c^2 at the Υ mass. These dimuon mass resolutions (the best among the LHC experiments) provide a clean separation of the different quarkonia states.

There is a slight dependence of the mass resolution on the event multiplicity. Increasing the multiplicity from $dN/d\eta = 0$ to 2500 degrades the mass resolution of the reconstructed Υ from 86 to 90 MeV/c^2.

Fig. 8 shows the opposite-sign dimuon mass distributions, for the high and low multiplicity cases and full acceptance ($|\eta| < 2.4$). The different quarkonia resonances appear on top of a continuum due to the various sources of decay muons: $\pi + K$, charm and bottom decays.

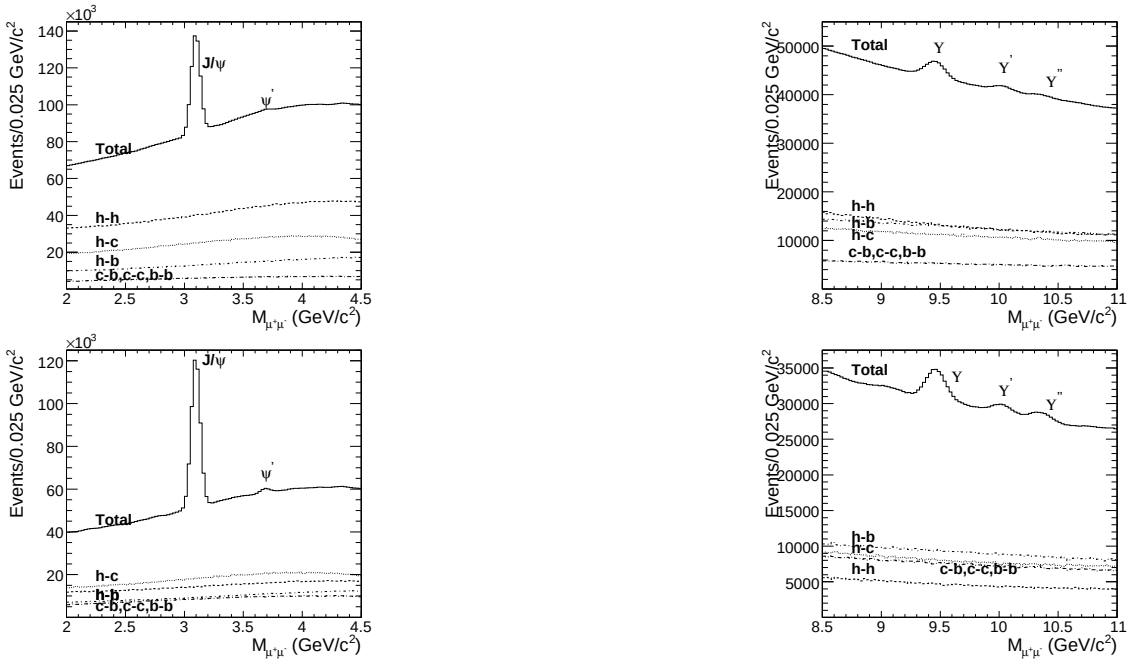

Figure 8: CMS detector. Dimuon mass distributions measured within $|\eta| < 2.4$ for Pb+Pb events with $dN_{ch}/d\eta = 5000$ (top) and $dN_{ch}/d\eta = 2500$ (bottom) in the J/ψ (left) and Υ (right) mass regions. The main background contributions are also shown: h, c and b stand for $\pi + K$, charm, and bottom decay muons, respectively.

Assuming that the CMS trigger and acceptance conditions treat opposite-sign and like-sign muon pairs equally, the combinatorial like-sign background can be subtracted from the opposite-sign dimuon mass distribution, giving us a better access to the quarkonia decay signals [3]. Fig. 9 shows the signal dimuon mass distributions, after background subtraction, for two different scenarios: $dN_{ch}/d\eta = 5000$ and $|\eta| < 2.4$ (worst case scenario); $dN_{ch}/d\eta = 2500$ and $|\eta| < 0.8$ (best case scenario).

The statistics of J/ψ and Υ, $\Upsilon^{'}$ and $\Upsilon^{''}$ with both muons in $|\eta| < 2.4$ region expected in one month of data taking are 140000, 20000, 5900 and 3500 correspondingly for the multiplicity $dN_{ch}/d\eta = 5000$ and 180000, 25000, 7300, 4400 for the multiplicity $dN_{ch}/d\eta = 2500$. The signal-to-background ratios are 0.6, 0.07 for J/ψ and Υ's for $dN_{ch}/d\eta = 5000$ correspondingly and 1.2, 0.12 for $dN_{ch}/d\eta = 2500$. The signal-to-background ratio (the number of events) collected in one month for the dimuons in J/ψ and Υ mass regions with both particles in $|\eta| < 0.8$ region are 2.75 (12600) and 0.52 (6000) for $dN_{ch}/d\eta = 5000$ and 4.5 (11600), 0.97 (6400) for $dN_{ch}/d\eta = 2500$. The background and reconstructed resonance numbers are in a mass interval $\pm\sigma$, where σ is the mass resolution.

These quantities have been calculated for an integrated luminosity of 0.5 nb^{-1} assuming an average luminosity $\mathcal{L}$ = 4×10^{26} cm^{-2}s^{-1} and a machine efficiency of 50%. The expected statistics are large enough to allow further offline analysis for example in correlation with the centrality of the collision or the transverse momentum of the resonance.

One has to remark, that taking into account hot matter interactions and assuming the same magnitudes as in RHIC, the J/ψ could be suppressed by a factor of three (including cold matter effects, but excluding regeneration possibility), while the background (both from heavy and light quark production) should decrease by a factor of from two to five depending on p_T for the accepted kinematical range [27]. Thus, the signal-to-background ratio at the J/ψ mass should increase anyway.

The J/ψ transverse momentum and rapidity distributions are shown in Fig. 10, at the generated and reconstructed levels, for the two different multiplicity scenarios. The corresponding distributions for the Υ are shown in Fig. 11.

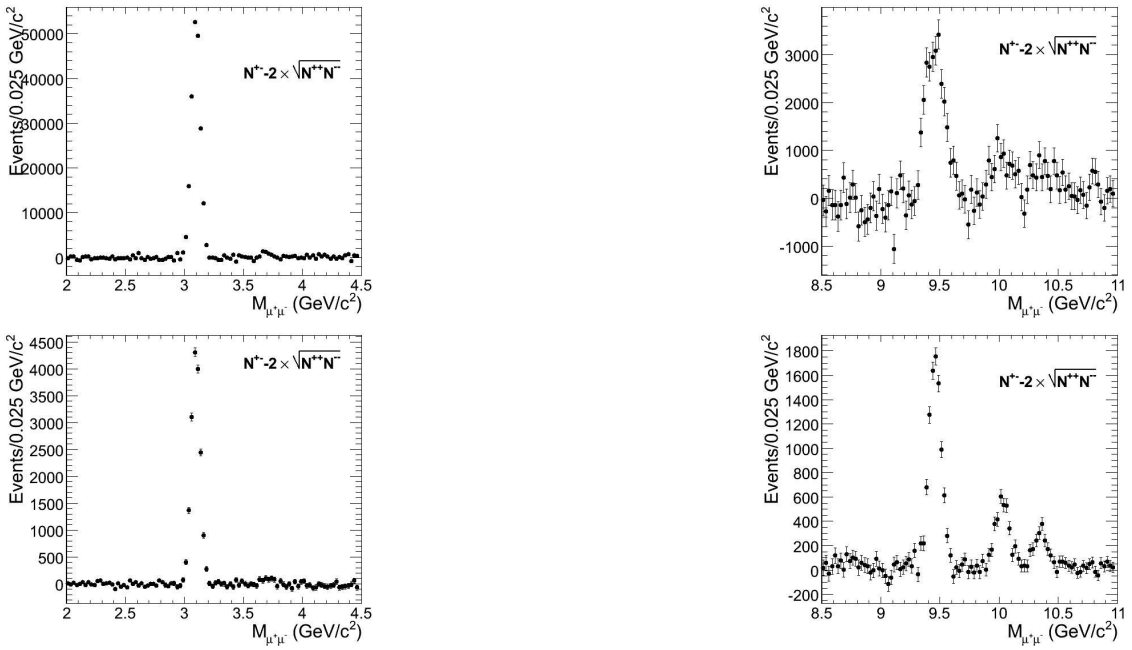

Figure 9: CMS detector. Signal dimuon mass distributions in the J/ψ (left) and Υ (right) mass regions, as expected after one month of Pb+Pb running (0.5 nb^{-1}). Top panels for $dN_{ch}/d\eta = 5000$ and $|\eta| < 2.4$ (worst case scenario), bottom panels for $dN_{ch}/d\eta = 2500$ and $|\eta| < 0.8$ (best case scenario); assuming no quarkonia suppression.

While the reconstructed Υ transverse momentum distributions have a shape quite similar to the generated one, a pronounced acceptance effect on the J/ψ spectrum is visible up to about 4 GeV/c, reflecting the J/ψ p_T acceptance curve (Fig. 7). The amount of statistics collected for the Υ resonance family in one nominal heavy-ion run with the high-level-trigger (HLT) settings discussed in [28] would allow one to study the p_T-dependence of the Υ' over Υ ratio, which is a very sensitive probe of the thermodynamical properties of the produced QGP [29].

4.3 CMS: Conclusions

With its $\approx 4\pi$ muon acceptance CMS can make very significant and, in some respects, unique contributions to quarkonia studies in heavy-ion collisions. Studies of the Υ family, from pp to Pb+Pb, as well as from peripheral to central collisions, is likely to be of great interest at the LHC.

The key issue for CMS is the muon reconstruction efficiency in the tracker under conditions of extreme occupancies expected in Pb+Pb collisions. The reconstruction efficiency is in the range from 90% to 84% for dimuons with both muons in $|\eta| < 0.8$ for event multiplicity up to $dN_{ch}/d\eta = 5000$. For muon pairs with at least one muon in the range $0.8 < |\eta| < 2.4$ the efficiency is 70% for multiplicity up to $dN_{ch}/d\eta = 2500$. The purity is kept above 80%. The Υ mass resolution is 56 MeV/c^2 for the dimuons with both muons within pseudorapidity range $|\eta| < 0.8$. For the entire pseudorapidity region $|\eta| < 2.4$, the Υ mass resolution is 85 MeV/c^2 while the J/ψ mass resolution is 35 MeV/c^2.

The large rapidity aperture of the CMS muon detector, as well as the precise tracking, result in high statistics and a very good separation between the Υ states. The higher masses of the Υ states favour their measurement in the barrel with the muon momentum detection threshold limited to 3 GeV/c. Assuming only cold matter effect of shadowing, the number of events for one month of data taking is high enough to provide a comparison between the several impact parameter bins and to carry out the study of the more differential analysis ($dN/d\eta$, dN/dp_T), which will contribute significantly to clarify the physics mechanisms behind the production (and destruction) of quarkonia states in high-energy nucleus-nucleus collisions.

5 Summary

ALICE, ATLAS and CMS experiments will study quarkonia production at the LHC. Quarkonium will be detected via both dielectron and dimuon channels and will be reconstructed in the wide range of pseudorapidity $|\eta| < 4$

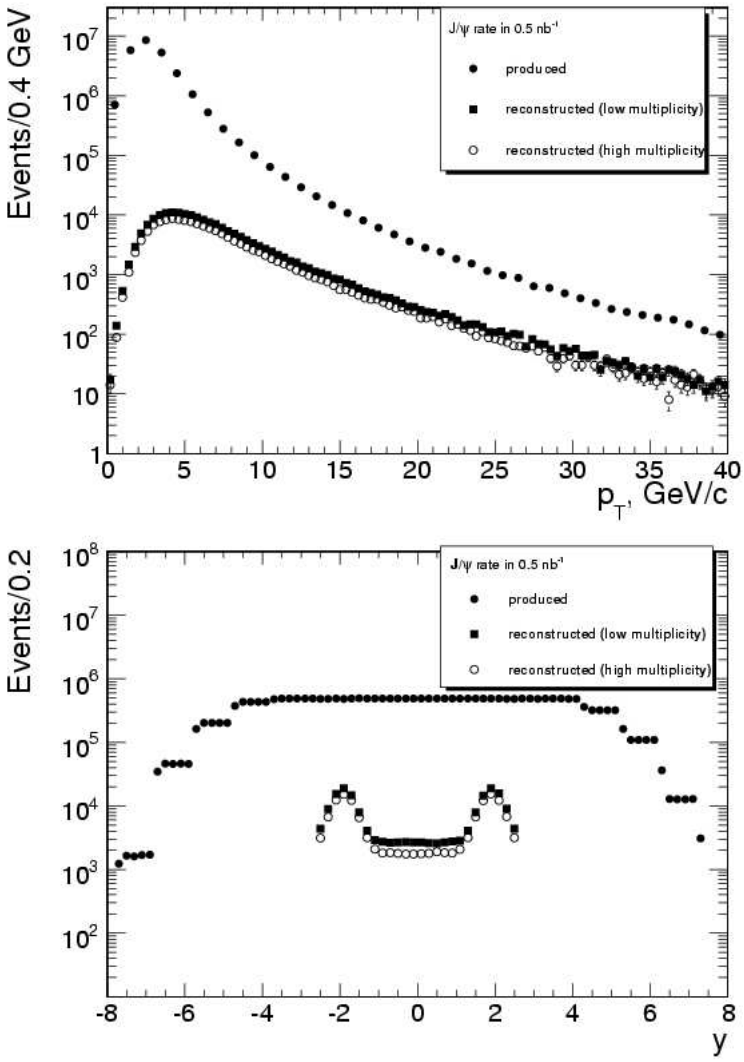

Figure 10: CMS detector. p_T (top) and rapidity (bottom) distributions of the muon pairs in the J/ψ mass peak for Pb+Pb at 5.5 TeV assuming no quarkonia suppression. The three distributions are the J/ψ's produced in 0.5 nb^{-1} (solid circles), and the reconstructed ones with either $dN_{ch}/d\eta = 2500$ (squares) or $dN_{ch}/d\eta = 5000$ (open circles).

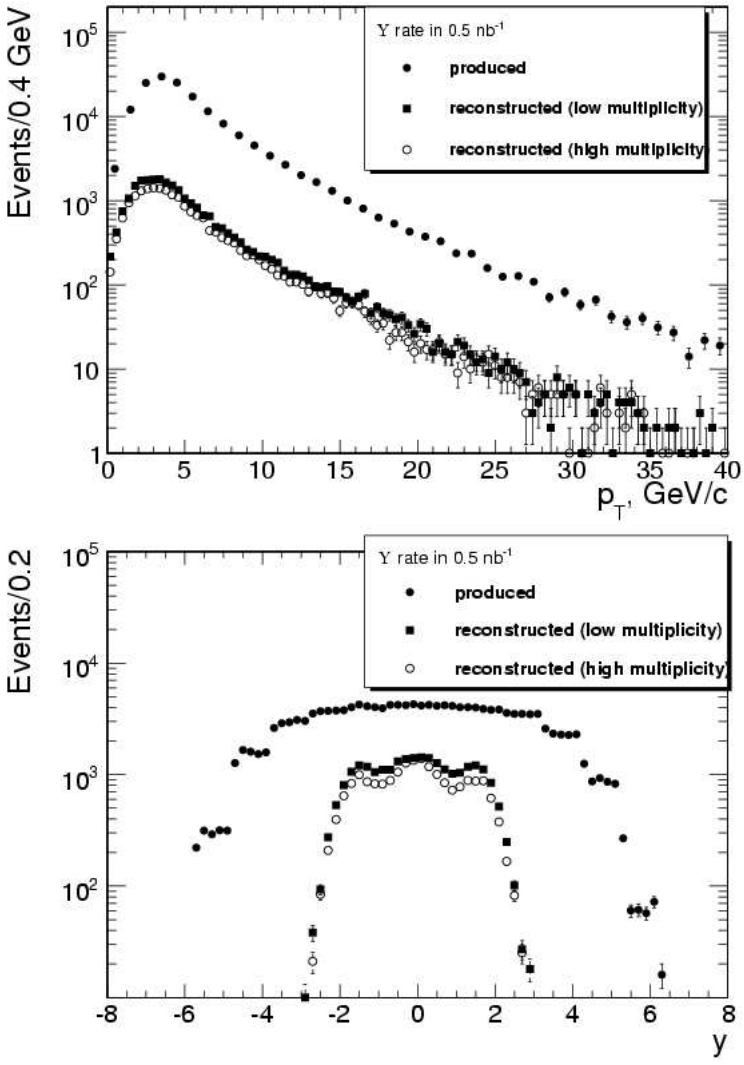

Figure 11: CMS detector. p_T (top) and rapidity (bottom) distributions of the muon pairs in the Υ mass peak for Pb+Pb at 5.5 TeV assuming no quarkonia suppression. The three sets of points correspond to: Υ's produced in 0.5 nb^{-1} (solid circles), reconstructed Υ's with $dN_{ch}/d\eta = 2500$ (squares), and reconstructed Υ's with $dN_{ch}/d\eta = 5000$ (open circles).

with excellent efficiency, purity and mass resolution. Full separation of Υ family will be possible.

6 Acknowledgments

The author wishes to express the gratitude to the members of ALICE, ATLAS and CMS collaborations for providing the materials and the organizers of Hard Probes 2008 conference for the warm welcome and the hospitality. The author also gratefully acknowledge support from Russian Foundation for Basic Research (grants No 08–02–08316 and No 08–02–91001) and Grants of President of Russian Federation for support of Leading Scientific Schools (No 1456.2008.2).

References

[1] Matsui, T. and Satz, H., Phys.Lett., **B178** (1986) 416.

[2] B. Alessandro et al., [NA50 Collaboration] Eur. Phys. J. **C39** (2005) 335.

[3] B. Alessandro et al., [NA50 Collaboration] Eur. Phys. J. **C49** (2007) 559.

[4] A. Adare *et al.* [PHENIX Collaboration], Phys. Rev. Lett. **98** (2007) 232301

[5] A. Adare *et al.* [PHENIX Collaboration], arXiv:0801.0220 [nucl-ex].

[6] R. Vogt, nucl-th/0507027.

[7] Karsch, Kharzeev and Satz, BNL-NT-05/50.

[8] L.Grandchamp and R.Rapp, Nucl.Phys. **A715** (2003) 545; hep-ph/0209141.

[9] *ALICE Physics Performance Report, vol. II*, CERN/LHCC 2005-030.

[10] G. Martinez, *ALICE potential for open heavy-flavour physics*, Proceedings Quark Matter 2006.

[11] *http://aliweb.cern.ch/offline/*

[12] Wolfgang Sommer et al., nucl-ex/0702045.

[13] B. Alessandro *et al.* [ALICE Collaboration], ALICE: Physics performance report, volume II, J. Phys. G **32** (2006) 1295.

[14] M.Gyulassy and X.-N. Wang, Phys.Rev. **D44** (1991) 3501.

[15] ATLAS Technical Design Report Volume 1, CERN-LHCC-99-14.

[16] ATLAS Technical Design Report Volume 2, CERN-LHCC-99-15.

[17] ATLAS heavy-ion Physics Letter of Intent, CERN-LHCC-2004-009.

[18] A. Lebedev [ATLAS Collaboration] in proceedings of Quark Matter'08.

[19] L. Rosselet et. al., ATLAS Analysis Note CERN-ATL-COM-PHYS-2008-002 (2008).

[20] *CMS HCAL Technical Design Report*, CERN/LHCC 97-31, 1997.

[21] *CMS MUON Technical Design Report*, CERN/LHCC 97-32, 1997.

[22] *CMS ECAL Technical Design Report*, CERN/LHCC 97-33, 1997.

[23] *CMS Tracker Technical Design Report*, CERN/LHCC 98-6, 1998.

[24] DAQ TDR CERN/LHCC/2002-26.

[25] M.Bedjidian, O.Kodolova, S.Petrushanko, CMS NOTE 1999/004.

[26] O.Kodolova, M.Bedjidian, J.Phys.G:Nucl.Part.Phys. **34** (2007) 143-175.

[27] B.I.Abelev et al., nucl-ex/0606003 v3.

[28] The CMS collaboration et al, *CMS TDR Addendum: High-Density QCD with heavy-ions*, J.Phys. G: Nucl.Part.Phys. **34** (2007) 2307-2455.

[29] Gunion, J. F. and Vogt, R., Nucl.Phys., **B492** (1997) 301.